

Fingerprint Recognition Technology with Ateb-Gabor Filtration

Mariya Nazarkevych ¹[0000-0002-6528-9867], Yaroslav Voznyi ¹[0000-0002-5481-9973],

Olha Mykich ¹[0000-0002-5190-8516], Michal Gregus ²[0000-0002-8156-8962]

Yaroslav Hnativ ¹[0000-0002-8011-8628] and Hanna Nazarkevych ³[0000-0002-6528-9867]

¹Lviv Polytechnic National University, 12 Bandery str., Lviv, 79013, Ukraine
mariia.a.nazarkevych@lpnu.ua

²Comenius University in Bratislava, Bratislava, Slovakia
Michal.Gregus@fm.uniba.sk

³Taras Shevchenko National University of Kyiv, 64/13, Volodymyrska Street, City of Kyiv, Ukraine, 01601 Kyiv, Ukraine,
h.nazarkevych@gmail.com

Abstract. The identification of fingerprints in the security information system is investigated. Fingerprint scanning was performed, papillae thinning was performed, Sherlock and Monroe fields were orientated, Ateb-Gabor filtration was performed, and three-dimensional Ateb-Gabor properties were investigated for different rational parameters. Their effect on filtering and subsequently on identification is revealed. Ateb-Habor filtering for biometric prints is applied, which significantly extends classic filtering by implementing a broader set of filters and providing a comprehensive approach to identification. The skeleton was executed using the Hilditch algorithm. The next step is to create the direction fields, using the method proposed by Sherlock and Monroe when forming the direction field of the papillary lines. Uses an average spine / trough nine pixels period. This imitates a sensor with the discriminability of 500 dpi. Frequency in areas decreases depending on position. The Hilditch algorithm generates a vector image. This image is in the form of a loaded graph - that is, found endpoints, points of intersection of the top of the graph and the lines and arcs of the edges of the graph.

Keywords: Fingerprint, identification, Gabor filtering.

1 Introduction

Fingerprint identification has become widely used lately. Various types of sensors — optical, capacities, ultrasonic and thermal — are used to obtain digital images of fingerprints. To date, the most common fingerprint imaging sensors are optical sensors.

There are two main categories of fingerprint comparison methods — the comparison of defined points and the comparison of the whole pattern of the fingerprint — a

template-on. The pattern identification method compares two images to see its resemblance. This method is typically used in fingerprint identification systems (show Fig.1). More commonly used technology is recognition based on point-by-point comparisons.



Fig. 1. Scanned fingerprints in bmp format

Minus thinning method for biometric images

Skeletonize algorithms are determined on consistent deletion of outline points. These points get rid of and the line becomes thinned out. The thinning algorithm is the removing of edge points where throughout the image moves mask 3×3 . These set of rules apply to every 3×3 window. Consider building a skeleton using the Hilditch algorithm (show Fig.2). The algorithm is designed to work with binary images. The algorithm is to scan the post-iterative pixel matrix of the image mask position and the consistent change of black pixels on white. The algorithm was described in [1].



Fig. 2. Application of the Hilditch algorithm to the prints shown in Fig. 1

2 Constructing a fingerprint with directions

To create the direction field, we use the method proposed by Sherlock and Monroe in forming the direction field of the papillary lines. As stated in [2], the description of minutia is classified as spine completion, bifurcation or divergent fork, application, convergence fork, inter junction or bridge, fragment or short spine, hook or spur, return, rejected interrupts, intersection, point, dashed spine [3].

The Sherlock and Monroe method was proposed in [4] to form the directional field of papillary lines. The model proposed by Sherlock and Monroe allows you to create a

direction field based on minute position information. The creation of papillary lines on the basis of the direction field and the density field is as follows: the original image containing some isolated singularities is gradually enlarged by the use of an Ateb-Gabor filter tuned to a certain density level.

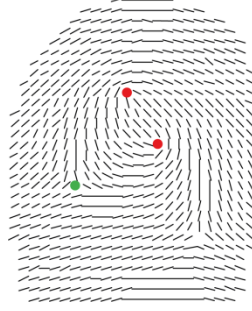


Fig. 3. Construction of the field of directions

The orientation model proposed by Sherlock and Monroe [5] provides an image of the orientation of the papillary lines taking into account the features of the nucleus and the delta of the fingerprint (show Fig.3). In this model, each element of the direction field is measured by its value. The local orientation of the papillary line is defined as the phase of the rational function module, is in the same location as the fingerprint nuclei and deltas (show Fig.4). The orientation for each point is determined by the formula:

$$O(z) = \frac{1}{2} \left[\sum_{i=1}^{n_d} g_{d_{si}}(\arg(z - d_{si})) - \sum_{j=1}^{n_c} g_{c_{sj}}(\arg(z - l_{sj})) \right], \quad (1)$$

where $g_k \alpha$ - functions defined for different deltas and nuclei

$k \in l_{s1}, l_{s2}, l_{snc}, \dots, d_{s1}, d_{s2}, d_{smd}$.

l_{sj} - j-e nuclei end d_{si} - i-delta in the complex plane [6].

The overall periodicity is selected consonant to the frequency distribution of the comb lines in actual fingerprints. Uses an average spine / trough period of nine pixels. This creates a sensor effect with a resolution of 500 dpi. Frequency in areas decreases depending on position.

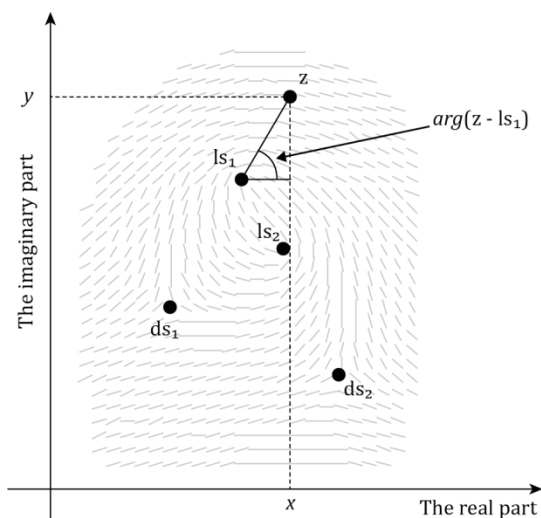


Fig. 4. Construction of a field of directions of orientation of papillary lines

The Sherlock and Monroe model is used as follows. The fingerprint is filtered by Ateb-Gabor. Further, thinning is carried out. The positions of nuclei and deltas are specified. A field of directions is built later.

2.1 Gabor filtering

Gabor wavelets are widely used for filtering fingerprints, and Gabor characteristics are recognized as the best representation for fingerprint recognition in terms of recognition factor. Moreover, it is demonstrated with resistance to changes in lighting and noise. When only one reference image is available per scanned image, they offer an adaptive weighted sub-Gabor's array for representing and recognizing fingerprints.

In [7], Gabor specifics were receiving for the classification of a classified representation. The main disadvantage of Gabor methods is the size of the Gabor function whose space is much larger as the images are collected by the Gabor filter bank. To solve this problem, the Adaboost algorithm and Entropy and Genetic Algorithms (GA) [8] are used to choose the most significant features of Gabor. But it is very difficult to choose the best method from the many Gabor features. [9]. In addition, the removal of Gabor's functions is very intensive, so these functions are not used for applications nowadays [10]. A simplified version of the Gabor wavelets was introduced in [11]. Unfortunately, Gabor simplified features are more sensitive to changes in lighting than original Gabor features.

Gabor filters are typically used for texture analysis, edge detection, feature extraction, unevenness estimation (in stereo), and more. Gabor filters include special classes of bandpass filters that pass a certain frequency band and reject others.

Images are filtered by Gabor filters in much the same way as conventional filters. We have a mask, the more precise term for it will be the "convolution core" that represents the filter. By mask we mean that we have a two-dimensional array. We use two-dimensional images. In these images, each pixel is assigned a weight value. The above array moves on each pixel of the image and performs a convolution operation. When applied to an image, the Gabor filter gives the greatest response at the edges and in places where the texture changes. The following images show the test image and its transformation after applying the filter.

The Gabor filter responds to changes in edges and textures. The filter responds well to the spatial location of the function. This occurs when coagulation kernels are applied in the spatial domain, in the frequency domains.

The method based on the application of the Gabor filter is quite simple and effective in constructing images of papillary lines. An iterative change of an input image containing one or more isolated sources causes the image to grow with local orientation. As a result, a consistent and very realistic picture of the papillary lines gradually emerges. In this case, in the random positions of the fingerprint appear minute different types.

2.2 Three-dimensional Ateb-Gabor filters

Gabor filtering [7] applies image modification. It is carried out by filtration, which is divided into the real and imaginary part. The real part of the Gabor filter kernel is realized by the cosine function. The imaginary part is constructed as a replacement of the cosine by the sine.

In this work we propose to use a Ateb-Gabor filtering to filter biometric fingerprints, which greatly expands classic filtering, implementing a wider set of filters and providing a comprehensive approach. Filtration [7] is described by the formula:

$$G(x, y, \lambda, \theta, \psi, \sigma, \varphi, m, n) = \exp\left(\frac{-x'^2 + \varphi^2 y'^2}{2\sigma^2}\right) \text{ca}\left(m, n, 2\pi \frac{x'}{\lambda} + \psi\right), \quad (2)$$

where

$$\begin{cases} x' = x \cos \theta + y \sin \theta \\ y' = -x \sin \theta + y \cos \theta. \end{cases}$$

where, φ - the parameter of data compression and scaling, σ - gaussian nucleus standart deviation; m, n - the rational numbers periodical Ateb-function; ψ - lagging; θ - parallel bandwidth of normal orientation; λ - the wavelength of the harmonic function. The filter results are shown in Fig. 5 - $m=9, n=0.5, \sigma=1, \theta=10 * \pi$, Fig. 6 - $m=3, n=5, \sigma=1, \theta=10 * \pi$, Fig. 7 - $m=3, n=7, \sigma=1, \theta=10 * \pi$, Fig. 8 - $m=3, n=11, \sigma=1, \theta=10 * \pi$.

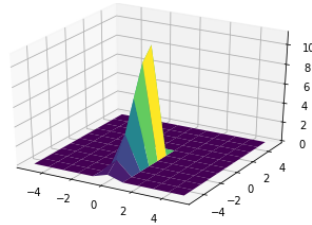


Fig. 5. Construction of three-dimensional Ateb-Gabor filter with rational numbers $m=9$, $n=0.5$,

$$\sigma=1, \theta = 10 * \pi$$

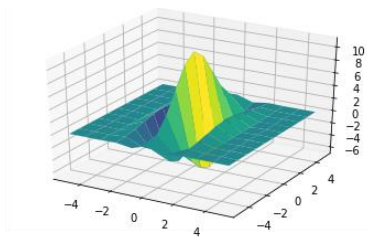


Fig. 6. Construction of three-dimensional Ateb-Gabor filter with rational numbers $m=3$, $n=5$, σ

$$=1, \theta = 10 * \pi$$

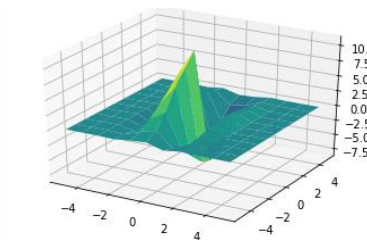


Fig. 7. Construction of three-dimensional Ateb-Gabor filter with rational numbers $m=3$, $n=7$, σ

$$=1, \theta = 10 * \pi$$

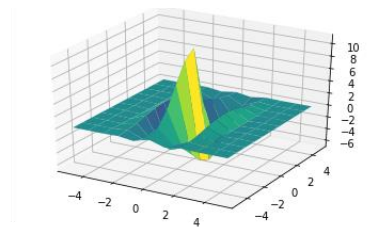


Fig. 8. Construction of three-dimensional Ateb-Gabor filter with rational numbers $m=3$, $n=11$,

$$\sigma=1, \theta = 10 * \pi$$

3 Skeletonize

Skeletonize transforms objects in images into a type of skeleton. This is distorted to represent the topology of the object by performing sequential image passages. Each time, pixel boundaries are identified and deleted, provided that they do not disrupt the object. Many skeletonization algorithms have been developed as an iterative sequential deletion of points on contours. Thinning algorithms, in particular Hilditch, work to eliminate boundary points so that the 3×3 window moves across the pixels of the image and the contents of the window apply the rules. Skeletonization works when sequentially scaling images and then removing pixels at the edge of an object. This lasts as long as there are no more pixels at the edge of the image. It works like a mask. The search table is then used to write to pixels of values 0, 1, 2, or 3 that are selectively deleted during iterations.

Thinning algorithms are considered in the work of Rutovitz [12], who first proposed the algorithm, which works as a definition of the intersection number, and allows you to perform parallel operations. This method can perform the entire tournament.

Another well-known algorithm is the Hilditch algorithm [13]. The wave algorithm is also known. It forms a vector image of the image in the form of a loaded graph - that is, the definition of endpoints, intersection points of the vertex of the graph, and arcs and lines bordering the edges of the graph.

And work with thin vector elements was developed in [14], which was complicated by latent elements that were poorly printable. The application of machine learning methods is devoted to the work [15], which is based on the training of data neural networks and the pre-filtering of images. And the work [16] describes the recognition in the video stream that is relevant and relevant to this study to change key images. The development of information technology for data transmission and optimization based on combinatorial methods is devoted to [17], where the optimization algorithms are taken. In [18, 19], the issue of image resolution enhancement, which took place when identifying finger biometric, was considered.

Fingerprint histogram alignment

Histogram alignment is a nonlinear process. Separating channels and aligning each channel individually is not a good way of leveling contrast. Alignment includes image intensity values, not color components.

This should be used to ensure that the intensity value is evenly balanced and does not in any way disturb the color balance. Therefore, the first step is to rebuild the color space from RGB into one of the color spaces, where the pixel intensity values are separated from the color components. The binarization results are shown in Figure 9. The initial image in grayscale is to the left Fig. 9a. In Figs. 9b shows an increase in counter-growth, 9c shows segmentation, which consists of splitting a digital image into several segments. This is done to simplify and change the presentation of the image to facilitate its analysis. In Figs. 9d shows local normalization, which is to bring the image back to the origin that is acceptable for recognition. In Figs. 9e shows a Gabor filter

transceiver. In Fig.10 show is image filtering: a - adding a processed image, b- binarization; c - median filtration; d- function extrac, e -filtered image.

If there are many colors in the image, the splitting method will cause a color imbalance. After the images were processed, they were subject to RSA encryption according to the algorithms [20, 21]. For grayscale images, work is devoted to the gray range [22]. In [23], a method for identifying biometric images is presented.

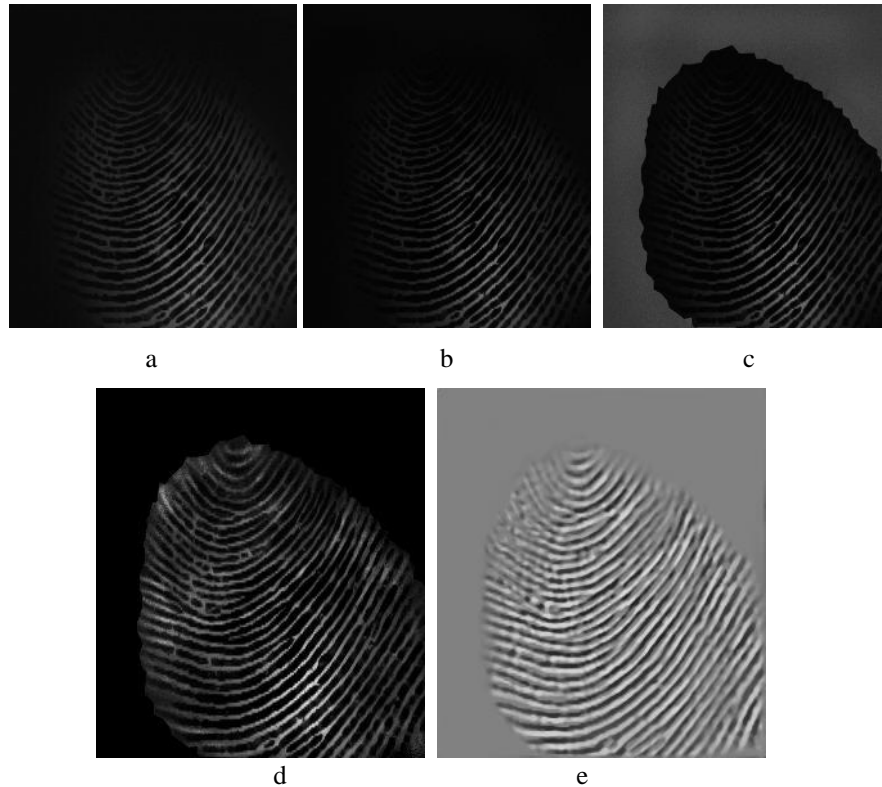


Fig. 9. Fingerprint histogram alignment: a Input image, b - Contrast enhancement; c – Segmentation; d - Local normalization; e - Gabor

Conclusions

Biometric fingerprints were identified and recognition was based on new filtering techniques. Biometrics were scanned, and papillae were thinned using the Hilditch algorithm. This method produces a vector representation of the image in the form of downloaded graphs. This is done to separate the end points, that is, the points of intersection of the top of the graph and the lines and arcs that contain the edges of the graph.

Field orientation was performed using the Sherlock and Monroe method. Ateb-Gabor-based filtering is implemented. Ateb-Gabor properties were investigated for various rational parameters and their effect on filtering was carried out.

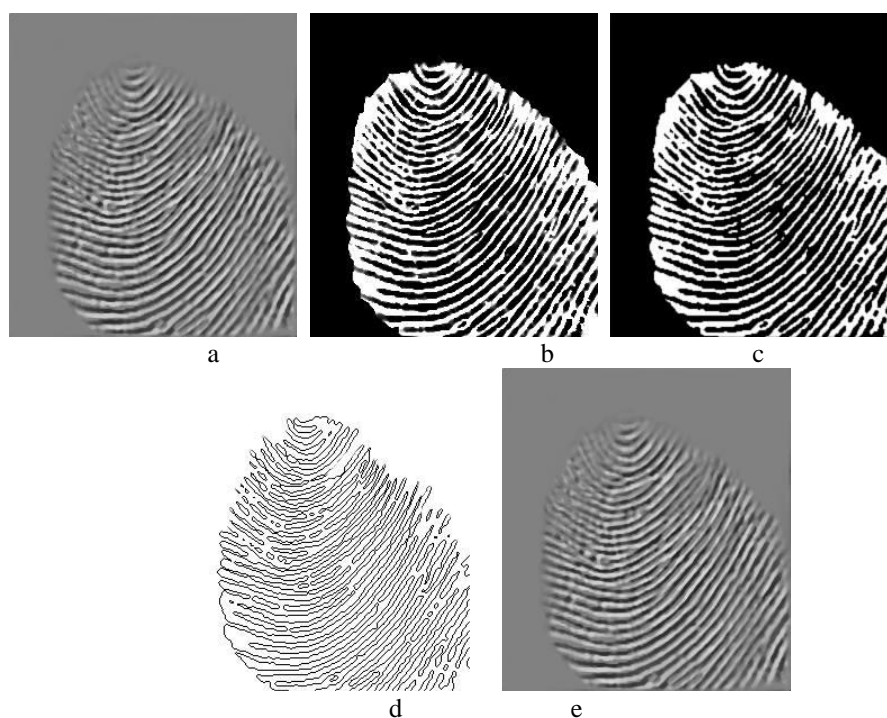


Fig. 10. Image filtering: a - adding a processed image, b-binarization; c - median filtration; d- function extrac, e -filtered image

References

1. Nazarkevych M., et. al.: Application perfected wave tracing algorithm. IEEE First Ukraine Conference on Electrical and Computer Engineering (UKRCON), Kiev, pp. 1011-1014. doi: 10.1109/UKRCON.2017.8100403. (2017).
2. Manickam, A., Devarasan, E., Manogaran, G., Chilamkurti, N., Vijayan, V., Saraff, S., ... Krishnamoorthy, R. Bio-medical and latent fingerprint enhancement and matching using advanced scalable soft computing models. *Journal of Ambient Intelligence and Humanized Computing*, 10(10), 3983-3995. (2019).
3. Stücker, M., Geil, M., Kyeck, S., Hoffman, K., Röchling, A., Memmel, U., & Altmeyer, P. Interpapillary lines—the variable part of the human fingerprint. *Journal of Forensic Science*, 46(4), 857-861. (2001).
4. Huckemann, S., Hotz, T., & Munk, A. Global models for the orientation field of fingerprints: an approach based on quadratic differentials. *IEEE Transactions on Pattern Analysis and Machine Intelligence*, 30(9), 1507-1519. (2008).
5. Vizcaya, P. R., Gerhardt, L. A. A nonlinear orientation model for global description of fingerprints. *Pattern Recognition*, 29(7), 1221-1231. (1996).

6. Kücken, M., Newell, A. C. A model for fingerprint formation. *EPL (Europhysics Letters)*, 68(1), 141. (2004).
7. Nazarkevych M. et. al.: Detection of regularities in the parameters of the ateb-gabor method for biometric image filtration. *Eastern-European journal of enterprise technologies*. № 1(2). pp. 57–65. (2019).
8. Shakeel, P. M., Tolba, A., Al-Makhadmeh, Z., Jaber, M. M. Automatic detection of lung cancer from biomedical data set using discrete AdaBoost optimized ensemble learning generalized neural networks. *Neural Computing and Applications*, 1-14. (2019).
9. Dronyuk I. ., et. al.: Gabor Filters Generalization Based on Ateb-Functions for Information Security. In: Gruca A., Czachórski T., Harezlak K., Kozielski S., Piotrowska A. (eds) *Man-Machine Interactions 5. ICMMI 2017. Advances in Intelligent Systems and Computing*, vol 659. Springer, Cham (2018).
10. Mishra, A., Dehuri, S. A Novel Hybrid FLANN-PsO Technique for real Time Fingerprint Classification. *Medico-Legal Update*, 19(2), 740-746. (2019).
11. M. Nazarkevych. et. al.: Image filtration using the Ateb-Gabor filter in the biometric security systems. XIV-th International Conference on Perspective Technologies and Methods in MEMS Design (MEMSTECH), Lviv, 2018, pp. 276-279. Doi: 10.1109/MEMSTECH.2018.8365749. (2018).
12. Chen, Chi-hau. *Handbook of pattern recognition and computer vision*. World Scientific, (2015).
13. Radhu Krishna, R. Enhanced skeletonization algorithm for fingerprint images. (2019).
14. Medykovskyy et. al.: Methods of protection document formed from latent element located by fractals. In 2015 Xth International Scientific and Technical Conference "Computer Sciences and Information Technologies"(CSIT). pp. 70-72. IEEE. (2015).
15. *Vasyl Lytvyn.*, et. al.: A Design of a recommendation system based on collaborative filtering and machine learning considering personal needs of the user. *Eastern-European journal of enterprise technologies*. Vol 4, No 2 (100). pp. 8–28. DOI: <https://doi.org/10.15587/1729-4061.2019.175507>. (2019).
16. Lytvyn V., et. al.: System Development for Video Stream Data Analyzing. In: Lytvynenko V., Babichev S., Wójcik W., Vynokurova O., Vysheymyrskaya S., Radetskaya S. (eds) *Lecture Notes in Computational Intelligence and Decision Making. ISDMCI 2019. Advances in Intelligent Systems and Computing*, vol 1020. Springer, Cham. (2019).
17. R. Oleg, K., et. al.: Information technologies of optimization of structures of the systems are on the basis of combinatorics methods. 12th International Scientific and Technical Conference on Computer Sciences and Information Technologies (CSIT), Lviv, 2017, pp. 232-235. doi: 10.1109/STC-CSIT.2017.8098776. (2017).
18. V.A. Mashkov, O. V. Barabash Self-checking and self-diagnosis of module systems on the principle of walking diagnosis kernel. *Engineering Simulation*, 1998, Vol.15, pp. 43-51. (1998).
19. Dmytro Peleshko et. al.: Image Superresolution via Divergence Matrix and Automatic Detection of Crossover. *International Journal of Intelligent Systems and Applications (IJISA)*, Vol.8, №.12, pp.1-8. DOI: 10.5815/ijisa.2016.12.01. (2016).
20. Kovalchuk, A., et. al.: Elements of RSA Algorithm and Extra Noising in a Binary Linear-Quadratic Transformations during Encryption and Decryption of Images. *Proceedings of the 2018 IEEE 2nd International Conference on Data Stream Mining and Processing*, pp. 542-544. (2018).
21. Rashkevych, Yu.Yu., et. al.: The use of disjunctive covering of images to increase strength of the RSA algorithm. 2011 Proceedings of 7th International Conference on Perspective Technologies and Methods in MEMS Design, pp. 168-169. (2011).
22. Anatoliy Kovalchuk, et. al.: An Approach towards an Efficient Encryption-Decryption of Grayscale and Color Images. The 6th International Symposium on Emerging Inter-networks, Communication and Mobility (EICM) , August 19-21, Halifax, Canada, pp. 630 – 635. (2019).
23. Nazarkevych M. et. al.: Complexity Evaluation of the Ateb-Gabor Filtration Algorithm in Biometric Security Systems, IEEE 2nd Ukraine Conference on Electrical and Computer Engineering (UKRCON), Lviv, Ukraine, 2019, pp. 961-964. (2019).